Pramana – J. Phys. (2017) 89:20
DOI 10.1007/s12043-017-1426-8

Influence of DC arc current on the formation of cobalt-based nanostructures

P B ORPE[1,2,*], C BALASUBRAMANIAN[1] and S MUKHERJEE[1]

[1]Facilitation Centre for Industrial Plasma Technologies, Institute for Plasma Research, A-10/B, G.I.D.C. Electronic Estate, Sector-25, Gandhinagar 382 016, India
[2]Department of Physical Science, Institute of Science, Nirma University, Sarkhej-Gandhinagar Highway, Ahmedabad 382 481, India
*Corresponding author. E-mail: prachi@ipr.res.in

MS received 10 November 2016; revised 21 January 2017; accepted 22 February 2017; published online 6 July 2017

Abstract. The synthesis of cobalt-based magnetic nanostructures using DC arc discharge technique with varying arc current is reported here. The structural, morphological, compositional and magnetic properties of these nanostructures were studied as a function of applied arc current. Various techniques like X-ray diffraction, transmission electron microscopy, EDAX and vibrating sample magnetometry were used to carry out this study and the results are reported here. The results clearly indicate that for a given oxygen partial pressure, an arc current of 100 A favours the formation of unreacted cobalt atomic species. Also change in arc current leads to variation in phase, diversity in morphology etc. Other property changes such as thermal changes, mechanical changes etc. are not addressed here. The magnetic characterization further indicates that the anisotropy in shape plays a crucial role in deciding the magnetic properties of the nanostructured materials. We have quantified an interesting result in our experiment, that is, for a given partial pressure, 100 A arc current results in unique variation in structural and magnetic properties as compared to other arc currents.

Keywords. Nanostructures; magnetism; thermal plasma; cobalt nanostructures.

PACS Nos 61.46.+w; 75.10.–b; 52.80.Mg

1. Introduction

Cobalt (Co) is a very interesting element with highest Curie temperature amongst all magnetic materials. Due to its enhanced magnetic properties even at nanoscale, cobalt and cobalt-based nanostructures have acquired widespread attention for its application in magnetic recording media [1–4], low power magnetic applications [5] and even biomedical applications [6,7]. The morphology of cobalt at nanoscale has been observed to have direct impact on magnetic properties [8]; enhanced coercivity is observed in nanowires of cobalt compared to spherical shaped nanoparticles [9]. Efforts are on to synthesize nanosized cobalt of various morphologies [10–12]. As a consequence, many synthesis techniques have been developed to improve and enhance magnetic properties of Co [13–16]. Thermal arc discharge is a technique for synthesizing various nanomaterials of different sizes and shapes of high purity and crystallinity by controlling different experimental parameters [17,18].

Recently, Co nanoparticles were synthesized using DC arc discharge and study of nucleation, growth and particle aggregation was carried out, for a single arc current [19]. However, the arc current has direct impact on the heat content in the system affecting its nucleation and growth. This has already been studied for other nanomaterials like AlN [20] in which lower arc currents lead to the formation of cubic phase of AlN while higher arc currents lead to the formation of hexagonal phase of AlN with a simultaneous formation of cubic phase.

In this paper, DC arc discharge technique has been used to synthesize Co-based nanopowders to study the influence of arc current on the structure, morphology and the composition and thus on magnetism.

2. Experimental procedure

For the synthesis of cobalt nanoparticles, commercial cobalt powder (Sigma Aldrich, 99.9%) is used as anode

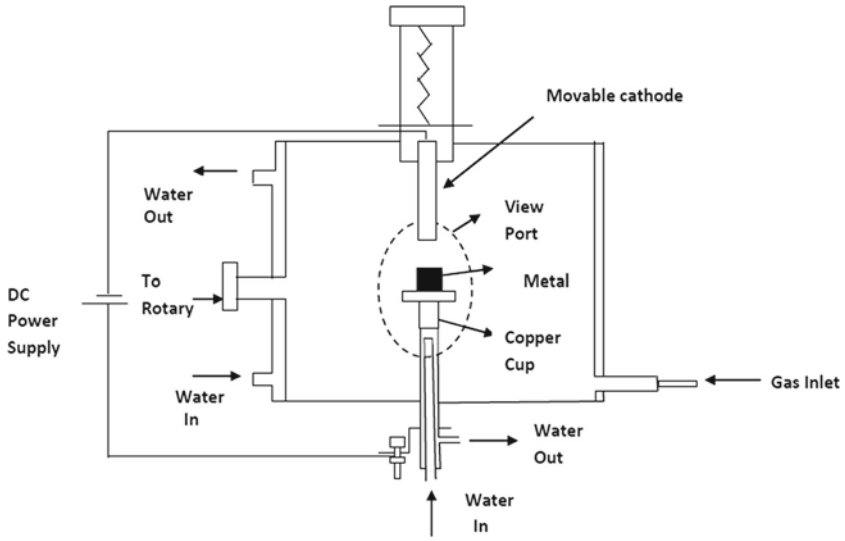

Figure 1. Schematic of the experimental set-up for the generation of nanoparticles.

material placed in crucible, while graphite rod of 10 mm diameter is used as the cathode. The experiments were performed with the arc current ranging from 50 to 150 A in steps of 50 A in helium (99.999% purity) ambient. For all the experiments, the synthesis chamber was initially evacuated to 3×10^{-2} mbar pressure and then filled with helium gas to atmospheric pressure. The base pressure was deliberately kept at low vacuum (mainly rotary pump vacuum) to study how oxidation levels change with arc current in the presence of low levels of oxygen. Experiments for currents higher than 150 A were not performed. A double-walled stainless steel chamber with movable cathode is used for these experiments. The chamber wall as well as anode holder are water cooled, the schematic of which is shown in figure 1. The chamber wall is cooled to create a steep temperature gradient and anode cooling is to prevent local heating of the anode. To start with, the movable cathode is brought in contact with the anode material and an arc is struck between the two electrodes. This results into the melting of the cobalt powder and further evaporation of the metal takes place. The metal vapour starts moving away from the plasma zone and formation of nuclei starts in the gas phase. In order to reduce the surface free energy, the growth of particles begins. The steep temperature gradient results in faster cooling and particles get condensed onto the wall of the chamber. These particles are scrapped off and taken for further characterization.

The structural analysis was carried out using X-ray diffraction (HT-Bruker, D8-Discover) in the range of 2θ varying from 10° to 80°. The transmission electron microscopy as well as EDAX (JEOL, JEM-2100) were carried out to study the morphology and composition of the Co nanostructures respectively. For TEM and EDAX, a small amount of cobalt nanopowder was dispersed in isopropyl alcohol and then dropped onto carbon coated copper grid. The magnetic measurements were carried out using vibrating sample magnetometry (ADE make, model EV9) technique.

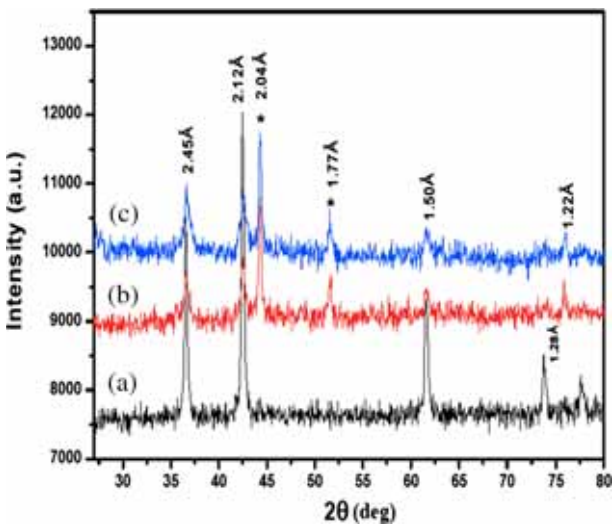

Figure 2. XRD pattern for cobalt-based nanostructures for arc currents (**a**) 50 A, (**b**) 100 A and (**c**) 150 A. (*-Unreacted Co).

3. Results and discussion

3.1 *X-ray diffraction studies*

The X-ray diffraction studies were carried out, as shown in figure 2, for phase analysis as well as for calculating

(a)

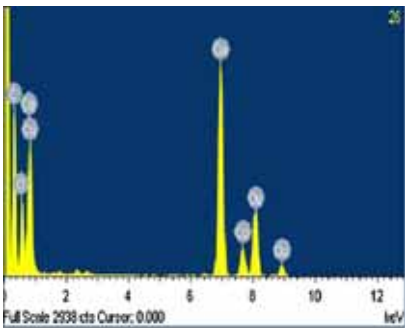

Element	Weight %	Atomic %
C K	37.00	63.91
O K	14.58	18.86
Co K	48.26	16.95

(b)

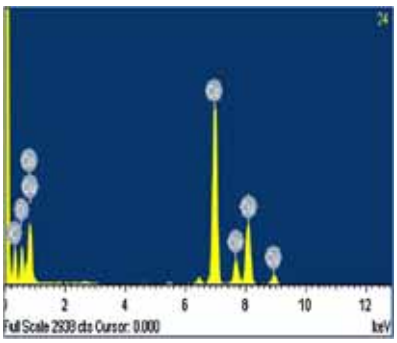

Element	Weight %	Atomic %
C K	12.76	34.47
O K	11.89	24.14
Co K	75.07	41.34

(c)

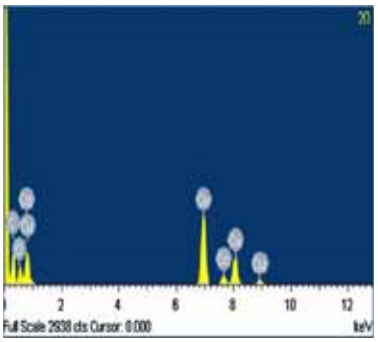

Element	Weight %	Atomic %
C K	26.06	53.50
O K	13.91	21.44
Co K	59.79	25.03

Figure 3. EDAX images for (**a**) 50 A, (**b**) 100 A and (**c**) 150 A are currents.

the average crystallite size of Co samples for three different arc currents.

For 50 A discharge current, *d*-spacing of 2.12 Å is the major peak, corresponding to (2 0 0) plane of the cubic phase of CoO (JCPDS No. 74-2392). Other peaks also match with the same phase, viz. CoO. As the discharge current is further raised to 100 A and 150 A in step of 50 A, additional peaks of 2.045 Å and 1.77 Å appear. These are characteristic peaks corresponding to the fcc phase of metallic cobalt (JCPDS-No. 15-0806) with (2 0 0) plane as the main peak and (1 1 1) plane as the additional peak of Co metal. In these spectra, 2.045 Å is the major peak for both the currents. The remaining peaks in 100 A and 150 A match CoO (JCPDS No. 74-2392) and as observed from figure 2, there is no evidence of this new phase of Co metal for 50 A discharge current. The formation of a mixed phase has been observed only for higher arc currents, viz. 100 A and 150 A. This is in line with the earlier reports on AlN forming multiple phases at higher currents compared to a single phase at lower current [20]. This is because, as the arc current increases from 50 A, the input power and heat generated due to this power also increase. This heat increases the rate of evaporation. As a result, Co metal atoms leave the liquid pool, forming a stable Co phase, while the remaining metal ions leaving the liquid pool react with

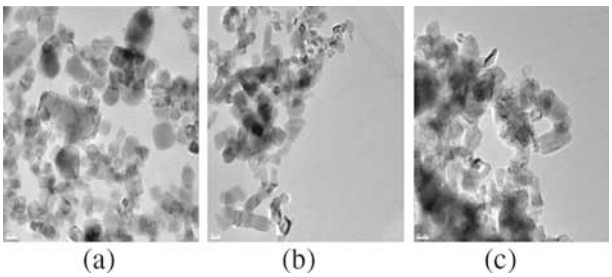

Figure 4. TEM images for (**a**) 50 A, (**b**) 100 A and (**c**) 150 A arc current.

oxygen ions present in the surrounding, forming a stable cobalt monoxide (CoO) phase. Therefore, unreacted Co metal phase is observed only for 100 A and 150 A arc current.

The average crystallite size calculated for 50 A, 100 A and 150 A is 29 nm, 30 nm and 38 nm respectively.

3.2 *EDAX analysis*

The EDAX analysis as shown in figure 3 was carried out to study the elemental proportion present in the samples. The Co:O atomic% ratio for 50 A is 0.89 of cobalt, for 100 A it is 1.71 of cobalt and for 150 A it is 1.16. It is observed that for 100 A arc current the atomic ratio% of Co:O is highest compared to 50 A and 150 A.

It can be inferred from EDAX characterization that the heat generated at 100 A discharge current is sufficient to form maximum number of cobalt metal atoms which further nucleate to form separate phase of cobalt along with cobalt monoxide. But in the case of 150 A discharge current, as the heat energy is high, the reaction probability of cobalt with oxygen outside the plasma zone increases. So there are unreacted species of cobalt but the atomic% ratio of cobalt in Co:O is lesser than that when the discharge current is 100 A. Still this ratio for cobalt atoms is higher than when the discharge current is 50 A because the high heat energy results in the generation of large atomic flux coming out of plasma zone with high velocity.

It is expected that a lower initial base pressure (lower than 3×10^{-2} mbar) would surely affect the outcome of the presence of oxygen and formation of cobalt oxide (for various arc currents) would reduce drastically or be completely eliminated. However, this study of the effect of base vacuum (from atmosphere to 10^{-5} mbar) on the oxidation is to be done separately and is not part of this paper.

3.2.1 *TEM analysis.* Transmission electron microscopy analysis is divided in two parts:

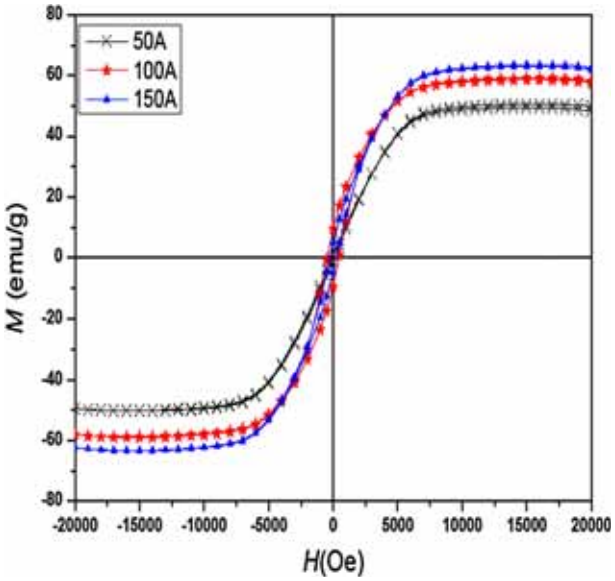

Figure 5. Hysteresis loops of Co samples at RT for three different arc currents.

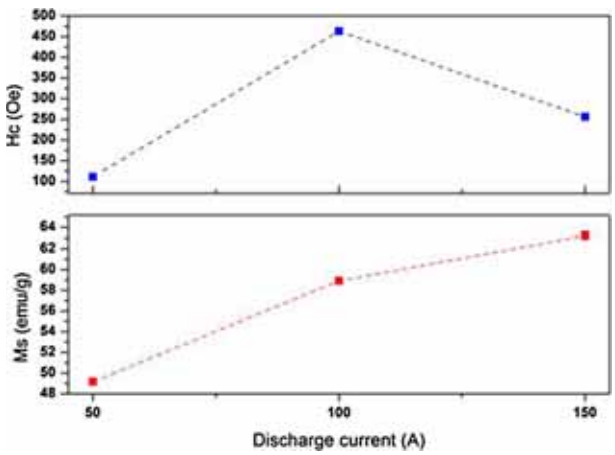

Figure 6. Plot showing variation of M_s and H_c with discharge current.

3.2.1.1 *Particle shape diversity*: In this analysis, study of variation in shapes of particles of cobalt-based nanostructures for the samples prepared with varying arc current is carried out. It has been observed that for 50 A discharge current most of particles are cubic while for 100 A and 150 A discharge currents there are diverse shapes such as rods and spheres apart from cubes. These shapes are shown in figures 4a–4c.

The diversity in the shape, as seen in figure 4, indicates that the discharge current increases the anisotropy in the particle shape. The particle shapes are mainly governed by the nucleation and growth mechanism. At the onset of homogeneous nucleation, in order to reduce the surface energy, the atoms from the supersaturated vapour state diffuse, forming nuclei. The growth of these nuclei

Table 1. M–H loop values from the curve.

Discharge current (A)	Coercivity H_c (Oe)	Saturation magnetization M_s (emu/g)	Squareness ratio (M_r/M_s)
50	111.21	49.1	0.02
100	462.94	58.9	0.16
150	255.87	63.2	0.07

occurs in the direction where the total energy of the system can be reduced [21]. When the arc current is low, viz. 50 A, there is lesser atomic flux leading to the formation of single-phase cobalt monoxide, as observed from the XRD pattern. CoO is found to have cubic symmetry. The particle shape evolving from the growth of crystals is also consequently found to be of cubic shape for 50 A arc current. Similar results are reported in [21], though for a different material and shape. But as the current increases to 100 A, the atomic flux as well as flux velocity increase compared to 50 A, leading to the diffusion of atoms from various directions forming multiphase components consisting of CoO as well as Co, resulting in the growth of nanoparticles of diverse shapes. Hence, various shapes such as rods and spheres are obtained, as observed in figure 4b. Further increase in the arc current to 150 A, leads to an increase in thermal energy resulting in the growth of totally anisotropic particle shapes.

3.2.1.2 *Particle size*: The particle sizes for 50 A, 100 A and 150 A range from 25 nm, 36 nm and 41 nm. The particle size is observed to increase by increasing arc currents. This is mainly due to a large number of ions coming out from the commercial cobalt powder with higher flux velocity, at higher arc currents resulting in the formation of bigger size clusters of particles, outside the plasma zone. These clusters of particles will continue to grow till thermal energy is available in the system but as these clusters get condensed onto the wall of the chamber, which is cooled by chilled water (10°C), this thermal energy is reduced and the formation of large size nanoparticles takes place at higher arc current. So the highest particle size distribution is obtained at 150 A.

Hence, we can infer that particle size is directly proportional to the arc current.

4. Study of magnetic properties

The magnetic properties for three samples have been investigated by studying the field dependence on the magnetization at room temperatures. In figure 5, M–H loop measurements in external field upto 20000 Oe are presented.

The saturation magnetization M_s is found to be the lowest for 50 A which is 49.1 emu/g. This could be mainly due to the fact that, as seen from XRD and EDAX, at 50 A the major phase formed is CoO, which is antiferromagnetic. The M_s value is found to further increase as the arc current increases, i.e. 58.9 and 63.3 emu/g for 100 A and 150 A, respectively, which is shown in figure 6. The coercivity value is found to be the highest for 100 A, viz. 463 Oe as compared to 50 A and 150 A which can be observed in figure 6. All these values of coercivity, saturation magnetization and squareness ratio are obtained from the hysteresis loop shown in figure 6 and reported in table 1. The squareness value is the M_r/M_s ratio. This value is the highest for 100 A current indicating that there is enhanced anisotropy in the particles [22].

The major reason for the highest squarness ratio found in the case of 100 A arc current is the presence of a large amount of Co, as confirmed from EDAX by atomic% of cobalt in Co:O ratio. Due to higher composition of metallic Co, the remanence magnetization for 100 A arc current is also highest, viz. 9.48 emu/g. So even after the removal of external magnetic field, the sample prepared at 100 A can retain its magnetization. For 50 A and 150 A, M_r is 1.11 emu/g and 4.78 emu/g, respectively.

5. Conclusion

The study illustrates that when the discharge current is kept at 100 A, a large quantity of unreacted Co is being synthesized along with CoO due to high temperature gradient and flux velocity at that particular discharge current. This probability of formation of larger quantity of Co atomic species for a particular current changes the morphology, stoichiometry, elemental composition [19] and thus affect the magnetic properties. It has been evaluated from the magnetic characterization data that the highest coercivity and remanence are also observed for 100 A arc current, making it more anisotropic.

It can be concluded from the experiments that there is a great influence of discharge current on the phase, morphology as well as composition and magnetic properties of the Co-based nanostructures synthesized using high thermal processing, i.e. arc discharge.

Acknowledgements

The authors acknowledge DST funding under Indo-Italian bilateral project for the work reported here. Authors also acknowledge Defence Metallurgical Research Laboratory, Hyderabad, for the magnetic characterization.

References

[1] D V Talapin, E V Shevchenko and H Weller, *Nanoparticles* (G Schmid, Wiley-VCH, Germany, 2004) p. 199
[2] C Petit, S Rusponi and H Brune, *J. Appl. Phys.* **95**, 4251 (2004)
[3] I-W Park, M Yoon, Y M Kim, Y Kim, J H Kim, S Kim and V Volkov, *J. Magn. Magn. Mater.* **272**, 1413 (2004)
[4] O Masala and R Seshadri, *Annu. Rev. Mater. Res.* **34**, 41 (2004)
[5] D Chiba, S Fukami, K Shimamura, N Ishiwata, K Kobayashi and T Ono, *Nat. Mater.* **10**, 853 (2011)
[6] C Osorio-Cantillo, A N Santiago-Miranda, O Perales-Perez and Y Xin, *J. Appl. Phys.* **111**, 07B324-3 (2012)
[7] Matthias Zeisberger, Silvio Dutz, Robert Muller, Rudolf Herget, Nina Matoussevitch and Helmut Bonnemann, *J. Magn. Magn. Mater.* **311**, 224 (2007)
[8] H T Zhu, J Luo, J K Liang, G H Rao, J B Li, J Y Zhang and Z M Du, *Physica B* **403**, 3141 (2008)
[9] An-Hui Lu, E L Salabas and F Schuth, *Angew. Chem. Int.* **46**, 1222 (2007)
[10] G Balaji, Rohini M Desilva, V Palshin, N Desilva, G Palmer and Challa S S R Kumar, *Mater. Sci. Eng. B* **167**, 107 (2010)
[11] Hwan-Gi Kim, Heon Lee, Byung Hoon Kim, Sun-Jae Kim, Ji-Myon Lee and Sang-Chul Jung, *Jpn J. Appl. Phys.* **52**, 01AN03-1 (2013).
[12] T Gnanavel and G Mobus, *J. Phys.: Conf. Ser.* **371**, 012047 (2012)
[13] M Mozaffari, J Amighian and E Darsheshdar, *J. Magn. Magn. Mater.* **350**, 19 (2014)
[14] M Green, *Chem. Commun.* **24**, 3002 (2005)
[15] S Peng, C Wang, J Xie and S Shouheng, *J. Am. Chem. Soc.* **128**, 10676 (2006)
[16] Cai-yin You, Z Q Yang, Q F Xiao, I Shorvanek, J Kovac, Z J Li, W Liu and Z D Zhang, *Eur. Phys. J. Appl. Phys*. **28**, 73 (2004)
[17] Haining Meng, Fangxia Zhao and Zhenzhong Zhang, *Int. J. Refractory Metals and Hard Mater*. **31**, 224 (2012)
[18] Ruslan Sergiienko, Etsuro Shibata, Akase Zentaro, Daisuke Shindo, Takashi Nakamura and Gaowu Qin, *Acta Mater.* **55**, 3671 (2007)
[19] S Hosseynizadeh Khezri, A Yazdani and R Khordad, *J. Ind. Eng. Chem.* **20**, 521 (2014)
[20] C Balasubramanian, V P Godbole, V K Rohatgi, A K Das and S V Bhoraskar, *Nanotechnol.* **15**, 370 (2004)
[21] Haolan Xu, Wenzhong Wang and Wei Zhu, *J. Phys. Chem. B* **110**, 13829 (2006)
[22] P Saravanan, R Gopalan, N V Rama Rao, M Manivel Raja and V Chandrasekaran, *J. Phys. D: Appl. Phys.* **40**, 5021 (2007)